

# Conditional Frechet Inception Distance

Michael Soloveitchik, Tzvi Diskin, Efrat Morin and Ami Wiesel

**Abstract**—We consider distance functions between conditional distributions functions. We focus on the Wasserstein metric and its Gaussian case known as the Frechet Inception Distance (FID). We develop conditional versions of these metrics, and analyze their relations. Then, we numerically compare the metrics in the context of performance evaluation of conditional generative models. Our results show that the metrics are similar in classical models which are less susceptible to conditional collapse. But the conditional distances are more informative in modern unsupervised, semisupervised and unpaired models where learning the relations between the inputs and outputs is the main challenge.

## I. INTRODUCTION

Generative models have revolutionized the machine learning world by learning how to efficiently sample from an unknown distribution. Such models have become ubiquitous since the introduction of the seminal Generative Adversarial Network (GAN) [1]. Conditional GANs were then developed to sample from a conditional distribution [2]. Recent unsupervised training of models can even learn from an unpaired dataset when the inputs and outputs are not aligned [3]–[6]. Every day new models are developed improving state of the art, such as speech-to-image translations [7]. Yet, it is still poorly understood how to measure their performance. There is a large body of works on unconditional metrics that help in optimizing and comparing different models [8] [9]. Among these, the Frechet Inception Distance [10] (FID) has become a standard measure due to its simplicity. Perhaps surprisingly, it is also frequently used in the analysis of conditional generators, e.g., [7], [11], [12]. The goal of this work is therefore to consider conditional versions of FID, develop the necessary machinery and examine it in different models and datasets.

Measuring the distance between two distributions is a fundamental problem in statistics. There are classical metrics based on likelihoods, divergences and other statistical notions, e.g. Kullback Leibler divergence (KLD) [13], Wasserstein distance (WD) [14], and total variation [14]. Each emphasizes various properties of the distributions with different sample and computational complexities. Unfortunately, modern applications involve huge dimensional datasets in which estimating these distances is difficult. Practical approaches consider simplified measures based on low dimensional embeddings, accuracy in some downstream task and/or some restricted parametric family. Arguably the most widely adopted metric in the computer vision literature is the Inception Score (IS) [15]. It is applicable for classification tasks and is based on the KLD of the labels. An improved version is the Mode Score which adds a diversity term to catch mode collapse problems [16]. Many metrics are designed to evaluate image quality. For example, LPIPS use

The authors are with The Hebrew University of Jerusalem, Israel . This research was funded by Center for Interdisciplinary Data Science (CIDR) in the Hebrew University, Israel.

learned features to measure the perceptual difference between two images [17]. SSIM uses correlations between the pixels of the images [18]. PSNR measures the peak signal to noise ratio between two monochrome images. Finally, one of the simplest and most popular metrics is FID which is based on an Inception embedding, and a particularization of WD to the simple case of multivariate normal distributions [10]. Recently, FID was also extended to mixture of Gaussians [19], [20].

Developing accurate and simple distances between conditional distributions is a more challenging problem. Instead of having two distributions, we now have two classes of distributions conditioned on a common input (feature). Most works simply ignore the conditioning and use unconditional metrics, e.g. [21], or combine FID measure with some other metric such as SSIM [22]. When the conditioning variables are discrete valued, it is natural and simple to resort to multiple unconditional metrics for each possible value [23]. In particular, Class Aware FID [24] and Intra-FID [25] improve unconditional FID by conditioning on the class labels. A main advantage of these metrics is their expressive power which generalized the Gaussian distribution with a Gaussian mixture assumption. When the inputs are continuous, e.g., in super-resolution or image translation tasks, this is clearly impossible. Recently, [26] proposed a conditional metric that measures consistency in the conditional low-resolution domain. Other related works tradeoff similar consistency measures with diversity metrics [27]. Also related is the Frechet Joint Distance (FJD) proposed in [28] which considers the distance to the joint distribution of the features and labels. FJD considers two different joint distributions, rather than two distributions conditioned on the same input.

The contribution of this paper is the introduction and analysis of conditional Wasserstein and FID metrics. We consider two versions of conditional distances as illustrated in Fig. 1. The model on the left is a classical unconditional distance between two marginal distributions. In the middle, we have two bivariate distributions that are restricted in their feature (conditioning) variable. In the right, we have a conditional model. Each of these graphical models leads to different Wasserstein and Frechet metrics.

Our main theoretical result is that the conditional metric is greater or equal to the restricted metric which is greater or equal to the marginal metric (which completely ignores the conditioning input). Practically, the conditional metrics can differentiate between two different distributions that have identical marginals. The conditional metric is more sensitive to these changes and we believe it should be preferred over the restricted version.

In order to enjoy the power of the conditional metrics, we derive closed form FID versions in the multivariate normal case. We evaluate these in the context of comparing generative

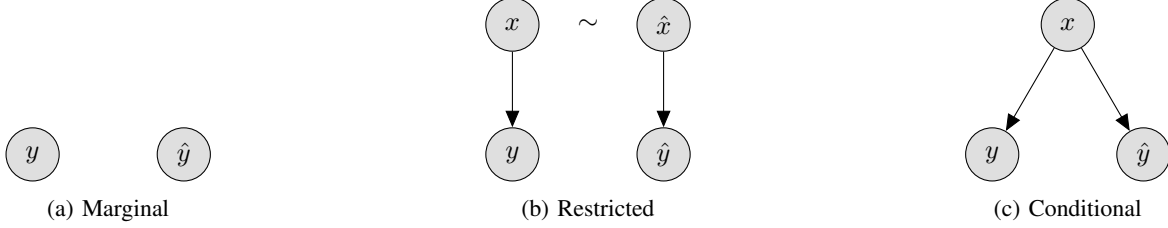


Fig. 1: Graphical Models. The tilde symbol  $\sim$  denotes  $p(x) = p(\hat{x})$ .

models. Initial experiments with classical supervised models resulted in similar FID and CFID values. Apparently, these models succeed in “squeezing out” all the information available in the paired inputs, and mostly differ in their output distributions as measured by FID. This led us to consider unsupervised or semisupervised models with additional marginal data. There, the main challenge is learning the relations between the inputs and outputs. FID is indifferent to these relations and is less useful in comparing such models. In contrast, CFID and RFID succeed in identifying these relations and provide a more informative comparison.

The paper is organized as follows. We begin in Section II where we introduce the marginal, restricted, conditional and joint Wasserstein metrics, and analyze their relations. Then, in Section III, we consider the Gaussian case and derive a closed form conditional FID (CFID). Finally, in Section IV, we illustrate the advantages of CFID over FID using numerical experiments with modern generative models.

Notations: We use blackboard fonts as  $\mathbb{P}$  to denote probability density functions. Due to space limitations,  $\mathbb{P}_z$  denotes  $\mathbb{P}_z(z)$  whenever it is not accompanied by a specific argument. For a positive semidefinite matrix  $C$ , the operator  $C^{\frac{1}{2}}$  denotes its squared root, namely a matrix with the same eigenvectors and the squared root eigenvalues. The trace operator is defined as  $\text{Tr}(A) = \sum_{i=1}^n A_{ii}$ . A diagonal matrix with elements  $v$  on the diagonal is denoted by  $\text{diag}(v)$ . Finally, the Dirac delta function  $\delta_d$  is an idealized point mass equal to zero everywhere except for zero and whose integral over the entire real line is equal to one.

## II. CONDITIONAL WASSERSTEIN

In this section, we define the conditional Wasserstein distance between two conditional distributions. Consider random variables  $\hat{y}$ ,  $y$  and  $x$ . Both  $y$  and  $\hat{y}$  are conditioned on the same  $x$  as illustrated in Fig. 1. Our goal is to develop a distance function between the distributions  $\mathbb{Q}_{y|x}$  and  $\mathbb{Q}_{\hat{y}|x}$  conditioned on  $x \sim \mathbb{Q}_x$ .

The conditional model induces the following distributions

$$\begin{aligned} \mathbb{Q}_{\hat{y},x} &= \mathbb{Q}_{\hat{y}|x} \mathbb{Q}_x \\ \mathbb{Q}_{y,x} &= \mathbb{Q}_{y|x} \mathbb{Q}_x \\ \mathbb{Q}_y &= \int \mathbb{Q}_{y,x} dx \\ \mathbb{Q}_{\hat{y}} &= \int \mathbb{Q}_{\hat{y},x} dx \end{aligned} \quad (1)$$

In this paper, we focus on the Wasserstein distance (WD) which has become the standard performance measure in gener-

ative models. This classical distance between two distributions is defined as:

$$\mathcal{W}(\mathbb{Q}_y; \mathbb{Q}_{\hat{y}}) = \min_{\mathbb{P}_{y,\hat{y}} \in \Pi(\mathbb{Q}_y; \mathbb{Q}_{\hat{y}})} \mathbb{E} [\|y - \hat{y}\|^2] \quad (2)$$

where  $\Pi$  is the set of joint distributions with prescribed marginals:

$$\Pi(\mathbb{Q}_y; \mathbb{Q}_{\hat{y}}) = \left\{ \mathbb{P}_{y,\hat{y}} \left| \int \mathbb{P}_{y,\hat{y}} dy = \mathbb{Q}_{\hat{y}}, \int \mathbb{P}_{y,\hat{y}} d\hat{y} = \mathbb{Q}_y \right. \right\}. \quad (3)$$

Specifically, in our context, we define the marginal WD as

$$\text{MWD} = \mathcal{W}(\mathbb{Q}_y; \mathbb{Q}_{\hat{y}}) \quad (4)$$

Before we turn to the conditional metric, it is instructive to define the WD between two joint distributions. This is straightforward by simply concatenating  $[y, x]$  and  $[\hat{y}, \hat{x}]$  and using  $\mathcal{W}(\mathbb{Q}_{y,x}; \mathbb{Q}_{\hat{y},\hat{x}})$ . We call it Joint Wasserstein Distance.:

$$\text{JWD} = \mathcal{W}(\mathbb{Q}_{y,x}; \mathbb{Q}_{\hat{y},\hat{x}}) \quad (5)$$

In the multivariate normal case, this is exactly the definition of FJD in [28].

In the context of conditional models, it makes sense to restrict the attention to the case in which  $x \sim \hat{x}$ , i.e.  $\mathbb{P}_x = \mathbb{P}_{\hat{x}}$ . This yields the Restricted Wasserstein Distance (RWD)

$$\text{RWD} = \mathcal{W}(\mathbb{Q}_{y,x}; \mathbb{Q}_{\hat{y},x}) \quad (6)$$

Finally, we introduce the conditional Wasserstein distance denoted by CWD. Given some  $x$ , one can use  $\mathcal{W}(\mathbb{Q}_{y|x}; \mathbb{Q}_{\hat{y}|x})$ . But this will result in a function of  $x$  which is a random variable. Therefore, we define CWD by taking an outer expectation with respect to  $x$ :

$$\text{CWD} = \mathbb{E}_x [\mathcal{W}(\mathbb{Q}_{y|x}; \mathbb{Q}_{\hat{y}|x})] \quad (7)$$

As expected, these metrics satisfy the following properties:

**Lemma 1.** *The Wasserstein distances satisfy*

$$\text{CWD} \geq \text{RWD} \geq \text{MWD}. \quad (8)$$

*Proof.* The full proof is provided in the appendix. Briefly, it is based on introducing an additional metric denoted by RWD3 such that  $\text{CWD} \geq \text{RWD3} \geq \text{RWD} \geq \text{MWD}$ . As their names suggest, CWD and RWD3 are both based on minimizations with respect to  $\mathbb{P}_{y,\hat{y},x}$ , whereas RWD relies on a minimization with respect to  $\mathbb{P}_{y,\hat{y},x,\hat{x}}$ . The inequalities are proved by comparing the different feasible sets in each of the distances.  $\square$

Lemma 1 emphasizes the importance of using CWD over MWD when comparing two conditional generative models.

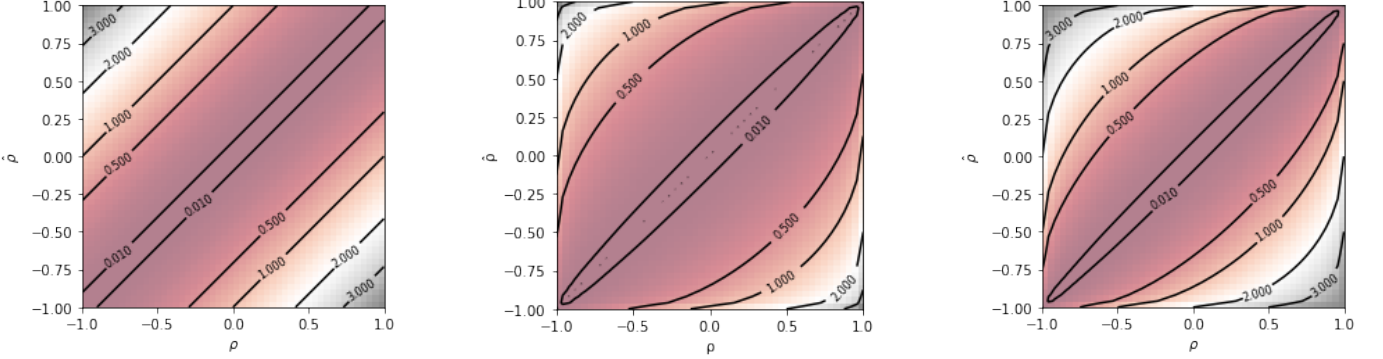


Fig. 2: Contours of different metrics:  $(\rho, \hat{\rho})^2$ ,  $\text{RFID}(\rho, \hat{\rho})$  and  $\text{CFID}(\rho, \hat{\rho})$ .

Two models may have zero MWD but be very different. For example, one of the models can completely ignore the conditioning and just shuffle the labels. On the other hand, if CWD is zero, then so is MWD and the models are identical.

### III. CONDITIONAL FRECHET INCEPTION DISTANCE

In practice, generative models are typically evaluated using a special case of MWD known as FID. FID is a successful approximation that tradeoffs sample and computational complexities with expressive power. First, it restricts the attention to multivariate normal marginals which involve only second order statistics. Second, it does not work directly with  $y$  and  $\hat{y}$ , but with their Inception embeddings which are hopefully of lower dimension and ‘‘more Gaussian’’. These nonlinear embeddings are critical in practice, but, for simplicity, we assume that the data was already embedded.

#### A. Derivation

The Gaussian distributions associated with Fig.1 are defined as

$$Q_{y|x}(x) = \mathcal{N}(m_{y|x}, C_{yy|x}) \quad (9)$$

$$Q_{\hat{y}|x}(x) = \mathcal{N}(m_{\hat{y}|x}, C_{\hat{y}\hat{y}|x}) \quad (10)$$

Both are conditioned on the same  $x$  distributed as

$$Q_x = \mathcal{N}(m_x, C_{xx}). \quad (11)$$

The conditional moments satisfy the identities [29]:

$$\begin{aligned} m_{y|x} &= m_y + C_{yx} C_{xx}^{-1} (x - m_x) \\ C_{yy|x} &= C_{yy} - C_{yx} C_{xx}^{-1} C_{xy} \end{aligned} \quad (12)$$

$$\begin{aligned} m_{\hat{y}|x} &= m_{\hat{y}} + C_{\hat{y}x} C_{xx}^{-1} (x - m_x) \\ C_{\hat{y}\hat{y}|x} &= C_{\hat{y}\hat{y}} - C_{\hat{y}x} C_{xx}^{-1} C_{x\hat{y}} \end{aligned} \quad (13)$$

The classical FID is simply defined using the marginals of  $y$  and  $\hat{y}$  and will be denoted as MFID in the rest of the paper, to emphasize that it a distance between the marginal distributions. After some algebraic manipulations, plugging these into MWD yields [10], [30]

$$\begin{aligned} \text{MFID} &= \|m_y - m_{\hat{y}}\|^2 \\ &+ \text{Tr} \left( C_{yy} + C_{\hat{y}\hat{y}} - 2 \left( C_{yy}^{\frac{1}{2}} C_{\hat{y}\hat{y}} C_{yy}^{\frac{1}{2}} \right)^{\frac{1}{2}} \right) \end{aligned} \quad (14)$$

Similarly, by defining

$$\begin{aligned} C_{(xy)(xy)} &= \begin{bmatrix} C_{xx} & C_{xy} \\ C_{yx} & C_{yy} \end{bmatrix} \\ C_{(x\hat{y})(x\hat{y})} &= \begin{bmatrix} C_{xx} & C_{x\hat{y}} \\ C_{\hat{y}x} & C_{\hat{y}\hat{y}} \end{bmatrix} \end{aligned} \quad (15)$$

RFID is given by

$$\begin{aligned} \text{RFID} &= \|m_y - m_{\hat{y}}\|^2 \\ &+ \text{Tr} (C_{(xy)(xy)} + C_{(x\hat{y})(x\hat{y})}) \\ &- 2 \text{Tr} \left( \left( C_{(xy)(xy)}^{\frac{1}{2}} C_{(x\hat{y})(x\hat{y})} C_{(xy)(xy)}^{\frac{1}{2}} \right)^{\frac{1}{2}} \right) \end{aligned} \quad (16)$$

Finally, CFID is the expected value of conditional FIDs as a function of  $x$ :

**Lemma 2.** *The conditional FID is given by*

$$\begin{aligned} \text{CFID} &= \mathbb{E}_x [\|m_{y|x} - m_{\hat{y}|x}\|^2] \\ &+ \text{Tr} \left[ C_{yy|x} + C_{\hat{y}\hat{y}|x} - 2 \left( (C_{yy|x}^{\frac{1}{2}}) C_{\hat{y}\hat{y}|x} (C_{yy|x}^{\frac{1}{2}}) \right)^{\frac{1}{2}} \right] \\ &= \|m_y - m_{\hat{y}}\|^2 + \text{Tr} [(C_{yx} - C_{\hat{y}x}) C_{xx}^{-1} (C_{xy} - C_{x\hat{y}})] \\ &+ \text{Tr} \left[ C_{yy|x} + C_{\hat{y}\hat{y}|x} - 2 \left( (C_{yy|x}^{\frac{1}{2}}) C_{\hat{y}\hat{y}|x} (C_{yy|x}^{\frac{1}{2}}) \right)^{\frac{1}{2}} \right] \end{aligned} \quad (17)$$

*Proof.* See appendix.  $\square$

As expected, it is easy to see that CFID is only a function of the second order statistics. It is zero if and only if  $m_y = m_{\hat{y}}$  as well as  $C_{yy} = C_{\hat{y}\hat{y}}$ ,  $C_{yx} = C_{\hat{y}x}$ .

#### B. Intuition

In order to gain more intuition on the different Frechet metrics, we plot them in a simple bivariate case. We consider two zero mean, unit variance, Gaussian distributions with different correlations. The output  $y$  is defined by

$$C = \begin{bmatrix} C_{xx} & C_{xy} \\ C_{yx} & C_{yy} \end{bmatrix} = \begin{bmatrix} 1 & \rho \\ \rho & 1 \end{bmatrix} \quad (18)$$

and its correlation with  $x$  is denoted by  $\rho$ . The output  $\hat{y}$  is defined similarly but with a correlation  $\hat{\rho}$ . In Fig. 2 we provide

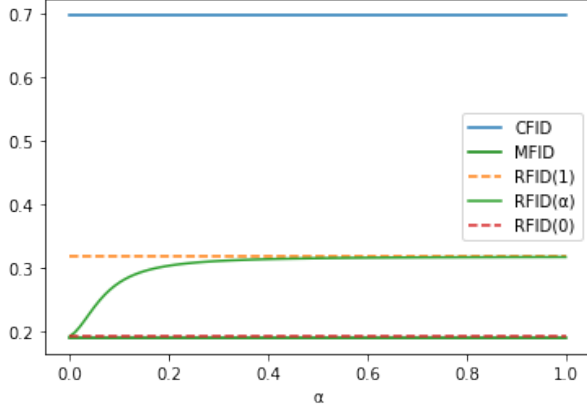


Fig. 3: MFID, RFID and CFID as function of  $\alpha$ .

contour plots of  $(\rho - \hat{\rho})^2$  (for reference), RFID and CFID, for different values of  $\rho$  and  $\hat{\rho}$ . It is easy to see that both distances behave similarly and differently from the squared metric. CFID is larger than RFID and is more sensitive to changes.

More insight on the differences between CFID and RFID can be obtained from the next lemma.

**Lemma 3.** *Assume  $x$ ,  $y$  and  $\hat{y}$  are zero mean random variables with a corresponding CFID. Consider a new triplet  $x_\alpha = \alpha x$ ,  $y$ , and  $\hat{y}$  in which  $x$  is scaled down by a deterministic  $0 < \alpha \leq 1$ . Then, the new distance  $CFID_\alpha$  is invariant to  $\alpha$  and is identical to CFID.*

*Proof.* See Appendix.  $\square$

The lemma shows an appealing property of CFID over RFID. As plotted in Fig. 3, CFID is invariant to scaling of  $x$ , whereas RFID collapses to MFID as we scale  $x$  towards zero. This agrees with the well known property that correlation coefficients are invariant to scalings of their random variables.

### C. Sample distances

In practice, we do not have access to the true distribution functions but use a dataset  $\mathcal{D} = \{x_i, y_i, \hat{y}_i\}_{i=1}^n$  where  $x_i$  is a conditioning feature vector,  $y_i$  is a true label and  $\hat{y}_i$  and a generated label. Estimating CFID given such a dataset is straight forward. Each of the second order moments in (12)–(13) is simply replaced by its empirical version, namely the corresponding sample means and same covariances. Compared to FID, RFID and CFID have computational and sample complexities of the same orders. Assuming equal dimensions for all the variables, these complexities roughly double.

## IV. EXPERIMENTS

In this section, we evaluate the different metrics via numerical experiments.

### A. Unsuccessful results in paired models

Before we delve into the details of our experiments, we briefly review a line of unsuccessful trials which we omitted from this paper. Initially, we began with intensive simulations

comparing conditional generators in different datasets. We compared various metrics including FID, CFID, IS, LPIPS, SSIM, PSNR and related metrics on downstream tasks. We expected that CFID would provide a better evaluation than FID, but both metrics typically behaved similarly. Apparently, all the models succeeded in “squeezing out” the information available in their paired inputs, and mostly differed in their output distributions as measured by FID. This led us to consider unsupervised or semisupervised models with additional marginal data. There, the main challenge is learning the relations between the inputs and outputs. In what follows, we report the results of these experiments.

### B. Synthetic parameter estimation

Our first experiment involves parameter estimation in a synthetic bivariate Gaussian model. The true distribution is zero mean, unit variance with correlation  $\rho$  as in (18). We experiment with algorithms that try to estimate this covariance given i.i.d. realizations  $z_i = [x_i, y_i]^T$  for  $i = 1, \dots, n$ . Given a  $2 \times 2$  covariance estimate  $\hat{C}$ , we define:

$$\hat{C} = \begin{bmatrix} C_{xx} & C_{x\hat{y}} \\ C_{\hat{y}x} & C_{\hat{y}\hat{y}} \end{bmatrix} \quad (19)$$

and discard the top left element  $C_{xx}$  which is not needed in test time. We compare three algorithms for estimating  $\hat{C}$ :

- Standard sample covariance (SC):

$$S = \frac{1}{n} z_i z_i^T \quad (20)$$

- Normalized sample covariance that knows  $C_{yy}$ . This is an idealized algorithm that assumes an additional dataset with an infinite number of unpaired samples  $\{y_j\}_{j=1}^\infty$  from which it can identify  $C_{yy}$ :

$$\begin{aligned} NSC_1 &= \text{diag}^{-\frac{1}{2}}(d_1) \cdot S \cdot \text{diag}^{-\frac{1}{2}}(d_1) \\ d_1 &= [1, S_{2,2}] \end{aligned} \quad (21)$$

- Normalized sample covariance that knows both  $C_{xx}$  and  $C_{yy}$ . This is an idealized algorithm that assumes two additional datasets with an infinite number of unpaired samples  $\{y_j\}_{j=1}^\infty$  and  $\{x_j\}_{j=1}^\infty$  from which it can identify both  $C_{yy}$  and  $C_{xx}$ .

$$\begin{aligned} NSC_2 &= \text{diag}^{-\frac{1}{2}}(d_2) \cdot S \cdot \text{diag}^{-\frac{1}{2}}(d_2) \\ d_2 &= [S_{1,1}, S_{2,2}] \end{aligned} \quad (22)$$

We compare these three estimators using MFID, RFID and CFID. The results are presented in Fig. 4. As expected,  $NSC_2$  has more information than its competitors and performs best under all criteria.  $NSC_1$  is the runner up and outperforms the naive SC estimator. In terms of metrics, CFID is most sensitive to this ranking, and RFID performs similarly. On the other hand, MFID ignores the conditional distributions and cannot compare  $NSC_2$  with  $NSC_1$ . Both result in an uninformative zero MFID. Altogether, this experiment clearly illustrates the benefits of using conditional metrics.

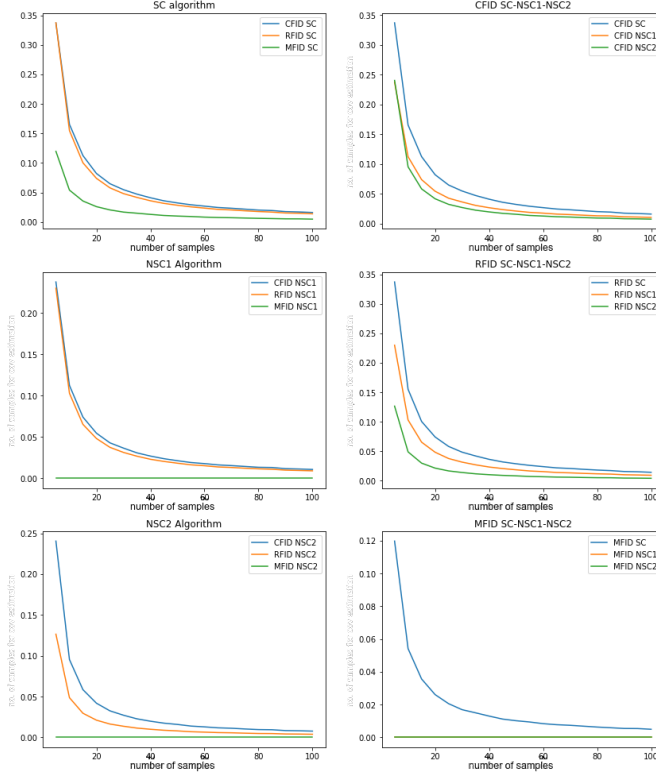


Fig. 4: MFID, RFID and CFID evaluations of SC, NSC1 and NSC2

### C. Paired vs unpaired generative models

In our second experiment, we use the metrics to compare four conditional generative models. The first two models are Pix2Pix [31] and BiCycleGAN [27]. These are trained in a paired (supervised) mode in which the training set consists of aligned pairs  $\{x_i, y_i\}$  of inputs and outputs. The next models, CycleGAN [3] and MUNIT [32], are unpaired (unsupervised) and rely on a dataset of inputs  $\{x_i\}$  and an additional unaligned dataset of outputs  $\{y_j\}$ . The unpaired models do not know which index  $i$  is associated with each index  $j$ . All the models are trained on PyTorch [27], with the default parameters over 60 epochs. For the FID embedding we used the last max-pool InceptionV3 layer [33].

First, inspired by the work of [4], we consider a rotation task which is known to be challenging for convolution networks. We use the CelebA [34] dataset with  $n = 30000$  samples, divided into a training set of size 20000 and a test set of size 10000. The results of the experiment are provided in Table I and Fig. 6. We also provide a few sample images of CycleGAN and Pix2Pix in Fig. 5. As expected and supported visually, all the models succeeded in learning  $\mathbb{Q}_y$ . The faces look reasonable and their FID values are similar and low. On the other hand, the unpaired CycleGAN and MUNIT failed in learning  $\mathbb{Q}_{y|x}$ . The output images of CycleGAN and MUNIT seem unrelated to their corresponding inputs and their CFID scores are significantly larger. Plotting CFID vs FID in Fig. 6 show that CFID can separate 'bad' models (CycleGAN and MUNIT) from the 'good' models (Pix2Pix and BiCycleGAN), whereas FID is indifferent to these qualities. As predicted by

Model	MFID	RFID	CFID
Pix2Pix	56.45	88.28	132.23
Cycle GAN	47.64	84.69	243.69
BiCycle GAN	<b>42.85</b>	<b>69.38</b>	<b>105.23</b>
MUNIT	53.65	146.54	265.37

TABLE I: Performance on CelebA.

Model	MFID	RFID	CFID
Pix2Pix	239.64	257.26	308.03
Cycle GAN	235.11	250.78	318.93
BiCycle GAN	<b>193.70</b>	<b>217.57</b>	<b>291.46</b>
MUNIT	232.72	252.09	317.60

TABLE II: Performance on Edges2Shoes.

the theory, RFID is somewhere in the middle. It identifies the advantages of BicycleGAN but gives a good score also to CycleGAN which is clearly a bad model.

Second, we repeat the experiment with the edges to natural image task based on the Edges2Shoes dataset [31]. The original dataset has only 300 examples in the test set, which is not enough to estimate the CFID. Therefore, we divided the original training set to a training set of size 35000 and a test set of size 10000. The results are provided in Table II and Fig. 7. Here too, the advantage of CFID over FID is evident. CFID clearly differentiates between the paired and unpaired models, and even shows a gap between Pix2Pix and BicycleGAN.

## V. DISCUSSION

In this paper, we considered conditional versions of the popular Wasserstein and Frechet distances. We proved that, among them, CWD and its applicable CFID version, lead to larger distances allowing for better differentiation between models. Practically, our experiments show that CFID is indeed useful in evaluating unpaired generative models, where the main challenge is learning the relation between the inputs and the outputs (rather than the marginal distribution of the outputs).

There are many directions for future work on conditional metrics. Most importantly, it is not clear what is truly a "good model" vs a "bad model". This also clearly depends on the underlying application, and specific downstream tasks. Therefore, it is not obvious how to illustrate or prove that conditional metrics are better. We hope future research will shed more light on this important topic. Furthermore, MFID, RFID and CFID are all clearly a crude approximation of reality, and ongoing work should consider better conditional distances suitable for non-Gaussian distributions.

## VI. APPENDIX

### A. Proof of Lemma 1

For convenience, we begin by recalling the definitions of the different distances:

$$\text{CWD} = \int \text{CWD}(x) \mathbb{Q}_x dx \quad (23)$$



Fig. 5: Visual results in CelebA. From left to right: input, ground-truth, BiCycle-GAN, Pix2Pix, Cycle-GAN and MUNIT

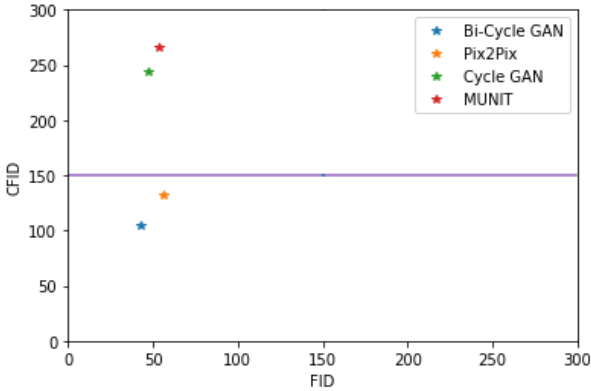


Fig. 6: MFID vs CFID in CelebA

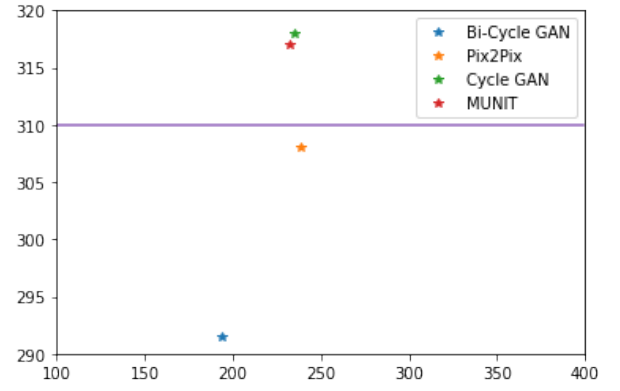


Fig. 7: MFID vs CFID in Edges2Shoes.

$$\text{CWD}(x) = \begin{cases} \min_{\mathbb{P}_{y, \hat{y}}} & \iint \|y - \hat{y}\|^2 \mathbb{P}_{y, \hat{y}} dy d\hat{y} \\ \text{s.t.} & \int \mathbb{P}_{y, \hat{y}} dy = \mathbb{Q}_{\hat{y}|x} \\ & \int \mathbb{P}_{y, \hat{y}} d\hat{y} = \mathbb{Q}_{y|x} \end{cases} \quad (24)$$

$$\text{RWD3} = \begin{cases} \min_{\mathbb{P}_{y, \hat{y}, x}} & \iiint \|y - \hat{y}\|^2 \mathbb{P}_{y, \hat{y}, x} dy d\hat{y} dx \\ \text{s.t.} & \int \mathbb{P}_{y, \hat{y}, x} dy = \mathbb{Q}_{\hat{y}, x} \\ & \int \mathbb{P}_{y, \hat{y}, x} d\hat{y} = \mathbb{Q}_{y, x} \end{cases} \quad (25)$$

$$\text{RWD} = \begin{cases} \min_{\mathbb{P}_{y,\hat{y},x,\hat{x}}} \int \int \int \int \left\| \frac{y - \hat{y}}{x - \hat{x}} \right\|^2 \mathbb{P}_{y,\hat{y},x,\hat{x}} dy d\hat{y} dx d\hat{x} \\ \text{s.t.} \quad \int \int \mathbb{P}_{y,\hat{y},x,\hat{x}} dy dx = \mathbb{Q}_{\hat{y},x}(\hat{y}, \hat{x}) \\ \quad \int \int \mathbb{P}_{y,\hat{y},x,\hat{x}} d\hat{y} d\hat{x} = \mathbb{Q}_{y,x}(y, x) \end{cases} \quad (26)$$

$$\text{MWD} = \begin{cases} \min_{\mathbb{P}_{y,\hat{y}}} \int \int \|y - \hat{y}\|^2 \mathbb{P}_{y,\hat{y}} dy d\hat{y} \\ \text{s.t.} \quad \int \mathbb{P}_{y,\hat{y}} dy = \mathbb{Q}_{\hat{y}} \\ \quad \int \mathbb{P}_{y,\hat{y}} d\hat{y} = \mathbb{Q}_y \end{cases} \quad (27)$$

Part 1: We begin by proving

$$\text{CWD} \geq \text{RWD3}$$

CWD involves an infinite number of optimization problems parameterized by  $x$ . We denote the optimal solution to  $\text{CWD}(x)$  by  $\mathbb{P}_{y,\hat{y}|x}^*$ . We then define

$$\mathbb{P}_{x,y,\hat{y}}^* := \mathbb{P}_{y,\hat{y}|x}^* \cdot \mathbb{Q}_x \quad (28)$$

We prove the inequality by showing that (28) is feasible for RWD3 and yields the same objective. For this purpose, note that it is a legitimate distribution

$$\int \mathbb{P}_{y,\hat{y},x}^* dy d\hat{y} dx = \int \left( \int \mathbb{P}_{y,\hat{y}|x}^* dy d\hat{y} \right) \mathbb{Q}_x dx = \int 1 \cdot \mathbb{Q}_x dx = \quad (29)$$

and feasible since

$$\int \mathbb{P}_{x,y,\hat{y}}^* d\hat{y} = \left( \int \mathbb{P}_{y,\hat{y}|x}^* d\hat{y} \right) \mathbb{Q}_x = \mathbb{P}_{y|x} \cdot \mathbb{Q}_x = \mathbb{Q}_{y,x} \quad (30)$$

$$\int \mathbb{P}_{x,y,\hat{y}}^* dy = \left( \int \mathbb{P}_{y,\hat{y}|x}^* dy \right) \mathbb{Q}_x = \mathbb{P}_{\hat{y}|x} \cdot \mathbb{Q}_x = \mathbb{Q}_{\hat{y},x} \quad (31)$$

Finally, it is easy to see that it gives the same objective value as CWD for:

$$\text{CWD} = \int \left( \int \int \|y - \hat{y}\|^2 \mathbb{P}_{y,\hat{y}|x}^*(y, \hat{y}) d(y, \hat{y}) \right) \mathbb{Q}_x(x) dx = \quad (32)$$

$$= \int \int \int \|y - \hat{y}\|^2 \mathbb{P}_{x,y,\hat{y}}^*(x, y, \hat{y}) dx dy d\hat{y} \quad (33)$$

Part 2: Next, we continue to prove

$$\text{RWD3} \geq \text{RWD}$$

RWD3 and RWD are very similar. The only difference is that RWD3 minimizes over  $\mathbb{P}_{y,\hat{y},x}$ , whereas RWD minimizes over  $\mathbb{P}_{y,\hat{y},x,\hat{x}}$ . To prove the inequality, we denote the optimal solution to RWD3 by  $\mathbb{P}_{y,\hat{y},x}^*$  and claim that

$$\mathbb{P}_{y,\hat{y},x,\hat{x}}^* = \mathbb{P}_{y,\hat{y},x}^* \delta_{x-\hat{x}} \quad (34)$$

is feasible for RWD and yields the same objective. Indeed, the delta function ensures that  $\int g(\hat{x}) \delta_{x-\hat{x}} d\hat{x} = g(x)$  for any function  $g$ . Therefore:

$$\left\| \frac{y - \hat{y}}{x - \hat{x}} \right\|^2 \cdot \delta_{x-\hat{x}} = \begin{cases} \|y - \hat{y}\|^2 & x = \hat{x} \\ 0 & x \neq \hat{x} \end{cases} \quad (35)$$

$$\int \int \mathbb{P}_{y,\hat{y},x}^* \delta_{x-\hat{x}} dy dx = \mathbb{Q}_{\hat{y},x} \quad (36)$$

$$\int \int \mathbb{P}_{y,\hat{y},x}^* \delta_{x-\hat{x}} d\hat{y} d\hat{x} = \mathbb{Q}_{y,x} \quad (37)$$

as required.

Part 3: Finally, it remains to show that

$$\text{RWD} \geq \text{MWD} \quad (38)$$

For this purpose, note that

$$\left\| \frac{y - \hat{y}}{x - \hat{x}} \right\|^2 \geq \|y - \hat{y}\|^2 \quad (39)$$

Thus, we can omit the squared norm associated with  $x - \hat{x}$ . Next, we denote the optimal solution to RWD by  $\mathbb{P}_{y,\hat{y},x,\hat{x}}^*$  and define

$$\mathbb{P}_{y,\hat{y}} = \int \int \mathbb{P}_{y,\hat{y},x,\hat{x}}^* dx d\hat{x} \quad (40)$$

This bivariate distribution is feasible for MWD and yields the same objective value as required.

### B. Proof of Lemma 2

This proof is quite technical and straight forward. We begin with the means:  $\mathbb{E}_x [\|m_{y|x} - m_{\hat{y}|x}\|^2] =$

$$= \mathbb{E}_x [\text{Tr} (m_{y|x} m_{y|x}^T - 2m_{y|x} m_{\hat{y}|x}^T + m_{\hat{y}|x} m_{\hat{y}|x}^T)] = \quad (41)$$

For the term  $\mathbb{E}_x [\text{Tr} (m_{y|x} m_{y|x}^T)]$ :

$$\begin{aligned} & \mathbb{E}_x [\text{Tr} ((m_y + C_{yx} C_{xx}^{-1} (x - m_x)) ((x - m_x)^T C_{xx}^{-1} C_{xy} + m_y^T))] = \\ & = \text{Tr} (0 + m_y \cdot m_{\hat{y}}^T + C_{yx} C_{xx}^{-1} C_{xx} C_{xx}^{-1} C_{xy} + 0) = \\ & = \text{Tr} (m_y \cdot m_{\hat{y}}^T + C_{yx} C_{xx}^{-1} C_{xy}) \end{aligned} \quad (42)$$

For the term  $-2\mathbb{E}_x [\text{Tr} (m_{y|x} m_{\hat{y}|x}^t)]$ :

$$\begin{aligned} & -2\mathbb{E}_x [\text{Tr} ((m_{\hat{y}} + C_{\hat{y}x} C_{xx}^{-1} (x - m_x)) ((x - m_x)^T C_{xx}^{-1} C_{x\hat{y}} + m_{\hat{y}}^T))] = \\ & = \text{Tr} (-2(0 + m_{\hat{y}} \cdot m_{\hat{y}}^T + C_{\hat{y}x} C_{xx}^{-1} C_{xx} C_{xx}^{-1} C_{x\hat{y}} + 0)) = \\ & = \text{Tr} (-2(m_{\hat{y}} \cdot m_{\hat{y}}^T + C_{\hat{y}x} C_{xx}^{-1} C_{x\hat{y}})) \end{aligned} \quad (43)$$

For the term  $\mathbb{E}_x [\text{Tr} (m_{\hat{y}|x} m_{\hat{y}|x}^T)]$ :

$$\begin{aligned} & \mathbb{E}_x [\text{Tr} ((m_{\hat{y}} + C_{\hat{y}x} C_{xx}^{-1} (x - m_x)) ((x - m_x)^T C_{xx}^{-1} C_{x\hat{y}} + m_y^T))] = \\ & = \text{Tr} (0 + m_{\hat{y}} \cdot m_{\hat{y}}^T + C_{\hat{y}x} C_{xx}^{-1} C_{xx} C_{xx}^{-1} C_{x\hat{y}} + 0) = \\ & = \text{Tr} (m_{\hat{y}} m_{\hat{y}}^T + C_{\hat{y}x} C_{xx}^{-1} C_{x\hat{y}}) \end{aligned} \quad (44)$$

Thus

$$\begin{aligned}
& \mathbb{E}_x [\text{Tr} ((m_y + C_{yx} C_{xx}^{-1} (x - m_x)) ((x - m_x)^T C_{xx}^{-1} C_{xy} + m_y^T)) = \\
& \mathbb{E}_x [\text{Tr} ((m_y m_y^T - 2 \cdot m_y m_{\hat{y}}^T + m_{\hat{y}} m_{\hat{y}}^T) + \\
& + (C_{yx} C_{xx}^{-1} C_{x\hat{y}} - 2 \cdot C_{yx} C_{xx}^{-1} C_{x\hat{y}} + C_{\hat{y}x} C_{xx}^{-1} C_{x\hat{y}}))] = \\
& \mathbb{E}_x [\|m_y - m_{\hat{y}}\|^2 + \\
& + \text{Tr} ((C_{yx} (C_{xx}^{-1} (C_{xy} - C_{x\hat{y}}))) + ((C_{yx} - C_{\hat{y}x}) C_{xx}^{-1}) C_{x\hat{y}}))] = \\
& \mathbb{E}_x [\|m_y - m_{\hat{y}}\|^2 + \\
& + \text{Tr} ((C_{yx} - C_{\hat{y}x}) C_{xx}^{-1}) C_{xy} - ((C_{yx} - C_{\hat{y}x}) C_{xx}^{-1}) C_{x\hat{y}})] = \\
& \|m_y - m_{\hat{y}}\|^2 + \text{Tr} ((C_{yx} - C_{\hat{y}x}) C_{xx}^{-1} (C_{xy} - C_{x\hat{y}})) \quad (45)
\end{aligned}$$

Now back to CFID, we conclude that:

$$\begin{aligned}
\text{CFID} = & \|m_y - m_{\hat{y}}\|^2 + \quad (46) \\
& + \text{Tr} [(C_{yx} - C_{\hat{y}x}) C_{xx}^{-1} (C_{xy} - C_{x\hat{y}})] \\
& + \text{Tr} \left[ C_{yy|x} + C_{y\hat{y}|x} - 2 \left( C_{yy|x}^{\frac{1}{2}} C_{\hat{y}\hat{y}|x} C_{yy|x}^{\frac{1}{2}} \right)^{\frac{1}{2}} \right]
\end{aligned}$$

### C. Proof of Lemma 3

To show that  $\text{CFID}_\alpha$  is invariant to its scaling, note that

$$\begin{aligned}
C_{x_\alpha x_\alpha} &= \alpha^2 C_{xx} \\
C_{x_\alpha y} &= \alpha C_{xy} \\
C_{yy|x_\alpha} &= C_{yy|x} \\
m_{y|x_\alpha} &= m_{y|x} \quad (47)
\end{aligned}$$

Therefore,  $\text{CFID}_\alpha = \text{CFID}$ .

## REFERENCES

- I. J. Goodfellow, J. Pouget-Abadie, M. Mirza, B. Xu, D. Warde-Farley, S. Ozair, A. Courville, and Y. Bengio, "Generative adversarial networks," *arXiv preprint arXiv:1406.2661*, 2014.
- M. Mirza and S. Osindero, "Conditional generative adversarial nets," *arXiv preprint arXiv:1411.1784*, 2014.
- J.-Y. Zhu, T. Park, P. Isola, and A. A. Efros, "Unpaired image-to-image translation using cycle-consistent adversarial networks," in *Proceedings of the IEEE international conference on computer vision*, 2017, pp. 2223–2232.
- E. Richardson and Y. Weiss, "The surprising effectiveness of linear unsupervised image-to-image translation," *arXiv preprint arXiv:2007.12568*, 2020.
- X. Huang, M.-Y. Liu, S. Belongie, and J. Kautz, "Multimodal unsupervised image-to-image translation," in *Proceedings of the European conference on computer vision (ECCV)*, 2018, pp. 172–189.
- K. Armanious, C. Jiang, S. Abdulatif, T. Küstner, S. Gatidis, and B. Yang, "Unsupervised medical image translation using cycle-medGAN," in *2019 27th European Signal Processing Conference (EUSIPCO)*. IEEE, 2019, pp. 1–5.
- J. Li, X. Zhang, C. Jia, J. Xu, L. Zhang, Y. Wang, S. Ma, and W. Gao, "Direct speech-to-image translation," *IEEE Journal of Selected Topics in Signal Processing*, vol. 14, no. 3, pp. 517–529, 2020.
- M. Lucic, K. Kurach, M. Michalski, S. Gelly, and O. Bousquet, "Are GANs created equal? a large-scale study," *arXiv preprint arXiv:1711.10337*, 2017.
- J.-T. Chien and C.-L. Kuo, "Variational bayesian GAN," in *2019 27th European Signal Processing Conference (EUSIPCO)*. IEEE, 2019, pp. 1–5.
- M. Heusel, H. Ramsauer, T. Unterthiner, B. Nessler, and S. Hochreiter, "GANs trained by a two time-scale update rule converge to a local nash equilibrium," *arXiv preprint arXiv:1706.08500*, 2017.
- S. Ravuri and O. Vinyals, "Classification accuracy score for conditional generative models," *arXiv preprint arXiv:1905.10887*, 2019.
- S. Zhou, M. L. Gordon, R. Krishna, A. Narcomey, L. Fei-Fei, and M. S. Bernstein, "Hype: A benchmark for human eye perceptual evaluation of generative models," *arXiv preprint arXiv:1904.01121*, 2019.
- Y. Rubner, C. Tomasi, and L. J. Guibas, "The earth mover's distance as a metric for image retrieval," *International journal of computer vision*, vol. 40, no. 2, pp. 99–121, 2000.
- C. Villani, *Optimal transport: old and new*. Springer Science & Business Media, 2008, vol. 338.
- T. Salimans, I. Goodfellow, W. Zaremba, V. Cheung, A. Radford, and X. Chen, "Improved techniques for training GANs," in *Advances in neural information processing systems*, 2016, pp. 2234–2242.
- T. Che, Y. Li, A. P. Jacob, Y. Bengio, and W. Li, "Mode regularized generative adversarial networks," *arXiv preprint arXiv:1612.02136*, 2016.
- R. Zhang, P. Isola, A. A. Efros, E. Shechtman, and O. Wang, "The unreasonable effectiveness of deep features as a perceptual metric," in *Proceedings of the IEEE conference on computer vision and pattern recognition*, 2018, pp. 586–595.
- Z. Wang, A. C. Bovik, H. R. Sheikh, and E. P. Simoncelli, "Image quality assessment: from error visibility to structural similarity," *IEEE transactions on image processing*, vol. 13, no. 4, pp. 600–612, 2004.
- P. Dimitrakopoulos, G. Sfikas, and C. Nikou, "Wind: Wasserstein inception distance for evaluating generative adversarial network performance," in *ICASSP 2020-2020 IEEE International Conference on Acoustics, Speech and Signal Processing (ICASSP)*. IEEE, 2020, pp. 3182–3186.
- A. Assa and K. N. Plataniotis, "Wasserstein-distance-based gaussian mixture reduction," *IEEE Signal Processing Letters*, vol. 25, no. 10, pp. 1465–1469, 2018.
- H. Alqahtani, M. Kavakli-Thorne, G. Kumar, and F. SBSSTC, "An analysis of evaluation metrics of GANs," in *International Conference on Information Technology and Applications (ICITA)*, 2019.
- S. You, N. You, and M. Pan, "Pi-rec: Progressive image reconstruction network with edge and color domain," *arXiv preprint arXiv:1903.10146*, 2019.
- N. Murray, "PfaGAN: An aesthetics-conditional GAN for generating photographic fine art," in *Proceedings of the IEEE/CVF International Conference on Computer Vision Workshops*, 2019, pp. 0–0.
- S. Liu, Y. Wei, J. Lu, and J. Zhou, "An improved evaluation framework for generative adversarial networks," *arXiv preprint arXiv:1803.07474*, 2018.
- T. Miyato and M. Koyama, "cGANs with projection discriminator," in *International Conference on Learning Representations*, 2018. [Online]. Available: <https://openreview.net/forum?id=ByS1VpgRZ>
- Y. Bahat and T. Michaeli, "Explorable super resolution," in *Proceedings of the IEEE/CVF Conference on Computer Vision and Pattern Recognition*, 2020, pp. 2716–2725.
- J.-Y. Zhu, R. Zhang, D. Pathak, T. Darrell, A. A. Efros, O. Wang, and E. Shechtman, "Toward multimodal image-to-image translation," in *Advances in Neural Information Processing Systems*, 2017.
- T. DeVries, A. Romero, L. Pineda, G. W. Taylor, and M. Drozdzal, "On the evaluation of conditional GANs," *arXiv preprint arXiv:1907.08175*, 2019.
- S. M. Kay, *Fundamentals of statistical signal processing*. Prentice Hall PTR, 1993.
- X. Ding, Z. J. Wang, and W. J. Welch, "Subsampling generative adversarial networks: Density ratio estimation in feature space with softplus loss," *IEEE Transactions on Signal Processing*, vol. 68, pp. 1910–1922, 2020.
- P. Isola, J.-Y. Zhu, T. Zhou, and A. A. Efros, "Image-to-image translation with conditional adversarial networks," in *Proceedings of the IEEE conference on computer vision and pattern recognition*, 2017, pp. 1125–1134.
- X. Huang, M.-Y. Liu, S. Belongie, and J. Kautz, "Multimodal unsupervised image-to-image translation," in *ECCV*, 2018.
- C. Szegedy, V. Vanhoucke, S. Ioffe, J. Shlens, and Z. Wojna, "Rethinking the inception architecture for computer vision," in *Proceedings of the IEEE conference on computer vision and pattern recognition*, 2016, pp. 2818–2826.
- Z. Liu, P. Luo, X. Wang, and X. Tang, "Deep learning face attributes in the wild," in *Proceedings of the IEEE international conference on computer vision*, 2015, pp. 3730–3738.